RSC Advances

PAPER

View Article Online
View Journal | View Issue

Cite this: *RSC Adv.*, 2025, **15**, 44517

Highly stable water-based dispersion of multilayer graphene modified with sodium dodecyl benzene sulfonate and polyacrylate terpolymer binder

Minghua Li, *[abc] Peng Wu,[ab] Honglin Chen,[ab] He Chu[ab] and Caicheng Liu[ab]

Received 3rd October 2025
Accepted 9th November 2025

DOI: 10.1039/d5ra07498c

rsc.li/rsc-advances

In this study, a facile and low-cost π–π non-covalent surface modification of commercial multilayer graphene (m-GR) was achieved by ball milling with an anionic surfactant (sodium dodecyl benzene sulfonate, SDBS) and a polyacrylate terpolymer binder (LA132) frequently used in lithium-ion batteries. Results from transmittance spectroscopy, zeta potential analysis, sedimentation photo, scanning electron microscopy (SEM), and atomic force microscopy (AFM) demonstrate that the modified m-GR exhibits good dispersion stability in water. Thermogravimetric analysis (TGA) confirms the successful adsorption of both modifiers onto the commercial m-GR surface. Importantly, while commercial m-GR is insoluble in water, the m-GRSL dispersion modified with 1.8 wt% SDBS and 20.0 wt% LA132 under the condition of a total 4 h ball milling time shows good aqueous dispersibility and long-term storage stability, maintaining no sedimentation for over one month. From an industrial perspective, this method is green and low-cost to achieve large-scale production.

1. Introduction

With the rapid development of consumer electronics and electric vehicle industries in recent years, the urgent demand for eco-friendly lithium-ion batteries has driven the elimination of *N*-methyl-2-pyrrolidone (NMP), a hazardous organic solvent widely used as the dispersion solvent in cathode slurry preparation.[1–5] The preparation of cathode slurry using water as the dispersion medium represents a critical step for sustainable lithium-ion batteries manufacturing. However, this shift requires water-based conductive slurries, such as graphene, which must overcome inherent hydrophobicity and aggregation tendency to prepare a stable dispersion in water.[6,7]

Graphene, renowned for its excellent electrical conductivity and high chemical stability,[8,9] is a promising conductive additive for water-based cathode slurry. However, it is challenging to disperse multilayer graphene (m-GR) in water due to the high surface area and strong van der Waals interactions between layers, and inherent hydrophobicity. One effective method is to prepare hydrophilic graphene dispersion by utilizing chemical oxidation modification. Unfortunately, the introduced defect sites during the process can affect the electrical conductivity. Furthermore, many works have been done to improve the wettability of graphene in water through facile non-covalent modification.[10] For example, Green *et al.* finished a detailed study comparing a series of pyrene derivatives for their ability to stabilise commercial graphene in water.[11] Wu *et al.* first prepared a dispersant solution by mixing polyvinyl pyrrolidone (PVP), sodium lauryl sulfate (SLS), and carboxymethylcellulose sodium (CMC) in water.[12] Then, the m-GR powder was added to the dispersant solution, stirred for 12 h, and sonicated for 15 min to make a graphene slurry for lithium-ion batteries. To utilize these excellent properties, commercial m-GR with lower price in market should be dispersed into water individually. However, water-based m-GR dispersion with good dispersibility, long storage stability and low production cost still presents a difficult challenge, as interlayer contact generates high van der Waals interaction energy.[8]

In recent years, most studies have focused on graphene dispersion *via* different non-covalent modications.[10–13] However, to obtain dispersions with higher graphene concentrations, larger concentrations of polymers and surfactants are required; this results in excess stabilizer in the dispersion and affect its electronic conductivity. Therefore, it is urgent to find a novel method to modify graphene dispersion as conductive slurry for lithium-ion batteries manufacturers. To meet conductivity requirements and enable mass production, stable graphene dispersion with good dispersibility and low production cost must be designed and developed.

In this work, we report a facile and low-cost π–π non-covalent surface modification of commercial multilayer GR (m-GR) by ball milling with an anionic surfactant (sodium dodecyl benzene sulfonate, SDBS) and a polyacrylate terpolymer binder (LA132) frequently used in lithium-ion batteries, as

[a]*School of Energy Materials and Chemical Engineering, Hefei University, Hefei, Anhui 230601, China. E-mail: liminghua@hfuu.edu.cn*

[b]*Anhui Provincial Engineering Research Center for Green Coatings High-performance Additives, Hefei, Anhui 230601, China*

[c]*Hefei Aigo Additives Technology Co.,Ltd, Hefei, Anhui 230601, China*

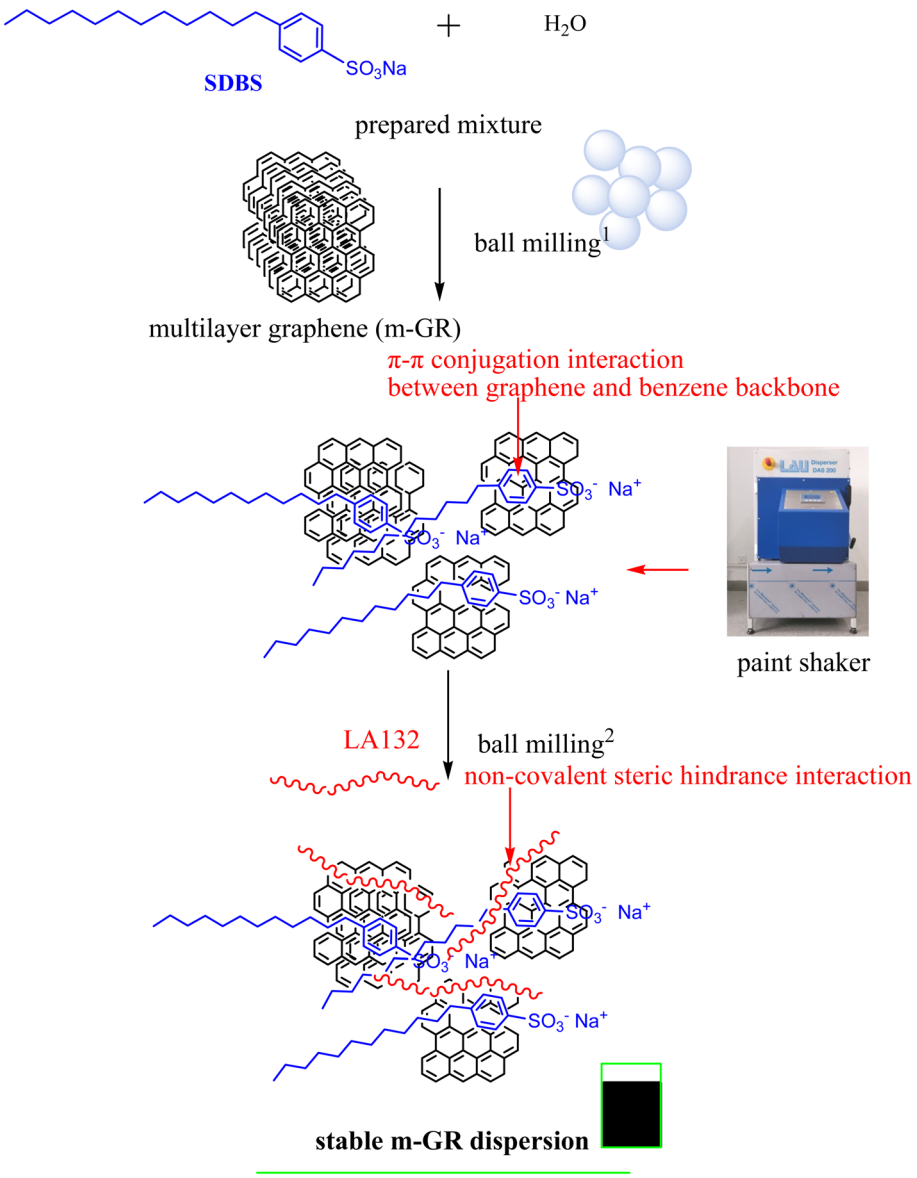

Fig. 1 The prepared route of highly stable water-based m-GR dispersion modified with sodium dodecyl benzene sulfonate and polyacrylate terpolymer binder.

shown in Fig. 1. We firstly select small molecule SDBS to disperse m-GR, since the negative charge of its sulfonate group can quickly influence the interaction between graphene and surfactant, and could have a positive effect on the stability of dispersion by π–π stacking between the benzene ring and graphene. Then, SDBS-modified m-GR can be easily modifed by using carboxylate and acrylate groups of LA132 to form hydrogen bonding. The long chains of macromolecule LA132 will enhance interfacial interactions between SDBS-modified m-GR and active materials in lithium-ion batteries, thereby improving compatibility. LA132 has two functions, namely it is both a macromolecule modifier for m-GR and a binder used in lithium-ion batteries.

Importantly, this method may enables the preparation of a stable modified m-GRSL dispersion with good dispersibility in water and good electronic conductivity in lithium-ion batteries, reported here for the first time. We further believe this work will accelerate the development of water-based lithium-ion batteries for new energy automobile applications.

2. Experimental

2.1 Materials

Commercial multilayer graphene (m-GR) (black powder, D_{50}/μm: 15–20, BET/m^2/g: 20–25, conductivity/S/cm: 600) was obtained from National Graphene Innovation Center (NGIC). The anionic surfactant sodium dodecyl benzene sulfonate (SDBS) and polyacrylate terpolymer binder (LA132) were purchased from Hefei Aigo Additives Technology Co. Ltd $LiFePO_4$ (LFP) and Super P bought from market were used without

purification. Deionized water was prepared using standard laboratory equipment.

2.2 Modification of m-GR

2.2.1 Modification of m-GR with SDBS. First, deionized water ((36 − n) g, n = 0.3, 0.6 and 0.9 g) and SDBS (n g) were added to a glass bottle, and stirred at 300 rpm for 15 min. After that commercial m-GR (4 g) and zirconia bead (80 g) were added to the preprepared mixture. The mixture was shaken for 3 h at room temperature using a paint shaker to yield uniform water-based dispersions (labeled m-GRS-1, m-GRS-2, and m-GRS-3, corresponding to n = 0.3, 0.6, and 0.9 g, respectively).

2.2.2 Modification of m-GR-*x* dispersion with LA132. Following the same experimental procedure, deionized water ((36 − n) g) and SDBS with the optimal content (n g) were added to a glass bottle, and stirred at 300 rpm for 15 min. After that commercial m-GR (4 g) and zirconia bead (80 g) were added to the preprepared mixture. The mixture was shaken for 3 h at room temperature in a paint shaker to obtain uniform water-based m-GRS-*x* dispersion.

Subsequently, LA132 (10 g) was then added to the pre-prepared m-GRS-*x* dispersion and shaken for an additional 1 h at room temperature to prepare a uniform and stable water-based m-GRSL dispersion. Finally, the m-GRS-*x* and m-GRSL powders were dried overnight at 80 °C under vacuum. In order to further illustrate the synergistic dispersion effect above, LA132 with the same content was also used to prepare m-GRL alone. The preparation procedure for the modified water-based m-GRSL dispersion is schematically illustrated in Fig. 1.

2.2.3 Preparation of cathode coating. The components of the cathodes include 80.0 wt% commercial LFP as active materials, 10.0 wt% conductive additives and 10.0 wt% polyacrylate terpolymer binder (LA132) binder. In order to prove the effect of modified m-GR on the electrochemical performance of the $LiFePO_4$ cathode, the electrodes with only Super P, as well as the mixture with 4 : 1 m-GR (m-GRSL) and Super P as conductive additives were prepared respectively. The slurry samples were labeled as LFP/SP-1, LFP-m-GR/SP-2 and LFP-m-GRSL/SP-3, respectively. The electrode slurry was prepared as follows: firstly, the LA132 was dissolved in water to get a uniform binder solution. Then, the conductive additives was added into the binder solution to form a mixture. Finally, the $LiFePO_4$ was added and then stired for 2 h. Finally, the mixture was coated uniformly on glass slide and dried under vacuum at 80 °C for 2 h.

2.3 Characterization

The UV-vis spectra of commercial m-GR and modified m-GR dispersions was analyzed using an ultraviolet-visible spectrophotometer (UV2600). Particle size distribution and zeta potential of the m-GR dispersions were characterized with a ZS90 particle size and zeta potential analyzer (Malvern, UK). Thermogravimetric analysis (TGA) of commercial m-GR and modified m-GR was performed under nitrogen atmosphere using a Netzsch 209F1 thermogravimetric analyzer, with a temperature range of 25–600 °C at a heating rate of 10 °C min^{-1}. The morphology of the m-GR dispersions was examined by field-emission scanning electron microscopy (FE-SEM, SU8010). Atomic force microscope (AFM, cypher) was used to test the thickness of the m-GR sheets. Electronical conductivity was measured by a HRMS-800 high temperature four probe resistivity tester.

3. Results and discussion

3.1 Size and distribution

The diluted water-based dispersion of commercial m-GR, modified m-GRS, m-GRL and m-GRSL with distinct Tyndall effect phenomenon was prepared for particle size and distribution analysis.[14] Based on the dynamic light scattering (DLS) technique, the number average diameter (D_{50}) and size distribution of water-based m-GR dispersions were shown in Fig. 2.

From Fig. 2(a), it is evident that the commercial m-GR exhibited poor dispersion in water, with serious agglomeration due to its high surface area, strong van der Waals forces, and intrinsic hydrophobicity.[15–17] Its average diameter (D_{50}) is about 824 nm as shown in Fig. 2(c). In contrast, the SDBS modified m-GRS showed good dispersibility in water, especially the m-GRS-3 dispersion (80 nm). This indicates that the dispersing effect of graphene using ball milling exfoliation in water can be enhanced by SDBS modification. Due to the new formed π–π conjugation interaction between graphene and benzene backbone of SDBS, the agglomeration was reduced effectively. With the increasing content of the SDBS modifier, the average diameter of graphene decreased gradually, especially the m-GRS-3 dispersion containg SDBS (n = 0.9 g) in Section 2.2. However, the m-GRS dispersion prepared with excessive SDBS was full of bubbles. Therefore, it is hard to obtain homogeneous and stable m-GR dispersion modified by different SDBS content, suggesting that non-covalent steric hindrance interaction of SDBS is still insufficient. To solve this problem, mixed modifiers including an anionic surfactant (SDBS) and a polyacrylate terpolymer binder (LA132) are used to modify commercial m-GR. Under optimized conditions, the D_{50} of the modified m-GRSL dispersion mixed with 1.8 wt% SDBS and 20.0 wt% LA132 under the condition of a total 4 h ball milling time reaches the value at 58 nm and shows good storage stability. To demonstrate the synergistic effect, m-GRL was also prepared using 20.0 wt% LA132 alone. In contrast, the average diameter (D_{50}) is about 410 nm as shown in Fig. 2(d). This indicates that the non-covalent steric hindrance provided by the LA132 macromolecule is also insufficient without the contribution of π–π conjugation.

3.2 UV-vis spectrum

From an industrial perspective, it is valuable to measure the optical transmittance of nanomaterials while providing rapid and reproducible indication of dispersion quality.[18,19] Fig. 3 shows the transmittance spectra of diluted commercial m-GR, modified m-GRS, m-GRL and m-GRSL dispersion with incident light wavelength ranging from 380 nm to 780 nm. We first compared the experimental data at 550 nm from commercial m-

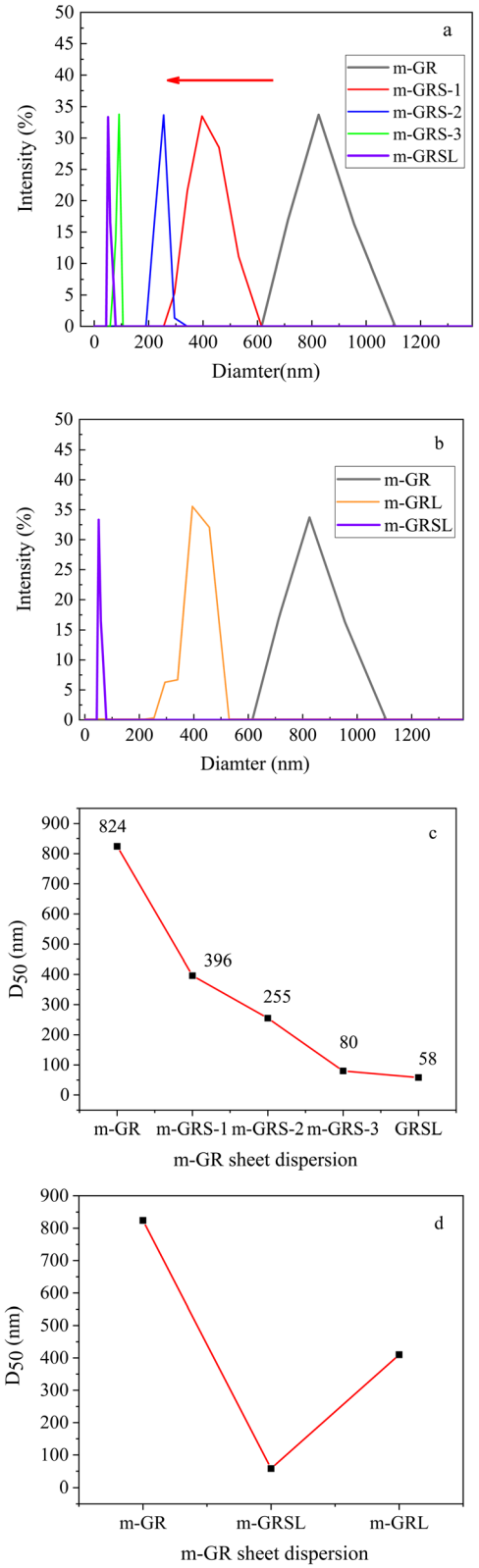

Fig. 2 Size and distribution (a and b) of commercial m-GR, modified m-GRS, m-GRL and m-GRSL dispersions. The data in the figure shows the average diameter (D_{50}) (c and d).

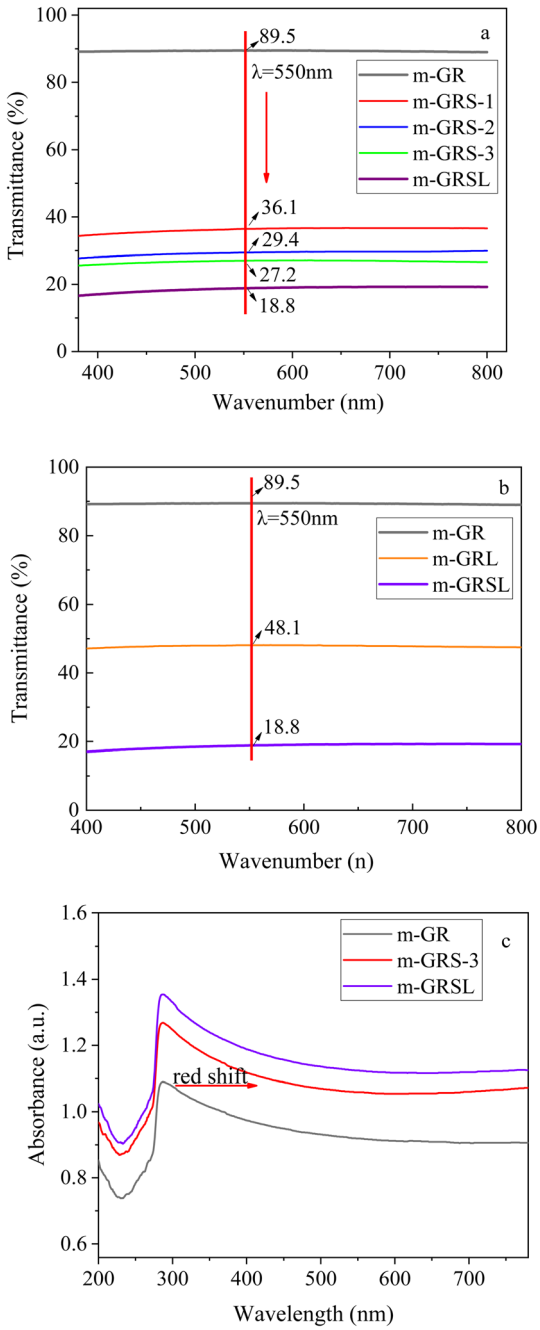

Fig. 3 Transmittance spectra (a and b) of commercial m-GR, modified m-GRS, m-GRL and m-GRSL dispersion with incident light wavelength ranging from 380 nm to 780 nm. The data in the figure shows the optical transmittance with incident 550 nm visible light. Absorbance spectra (c) of commercial m-GR, modified m-GRS-3 m-GRSL dispersion. Diluent concentration of graphene in all samples is 0.01 mg mL^{-1}. Commercial m-GR dispersion prepared using similar technology in Section 2.2 has the same solid content.

GR, m-GRS modified with different SDBS content. It can be seen that the modified m-GRS dispersions exhibit different optical transmittance in water.

Compared to 89.5% at 550 nm of commercial m-GR dispersion, the optical transmittance of the modified m-GRS

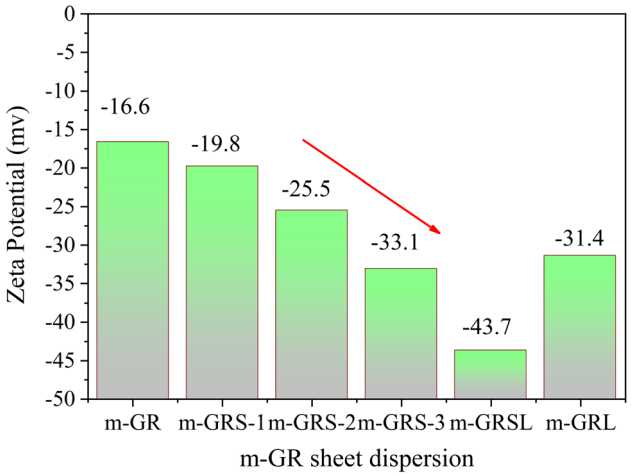

Fig. 4 Relation between zeta potential and water-based m-GR dispersion modified by different modifiers. Diluent concentration of graphene in all samples is 0.01 mg mL^{-1}.

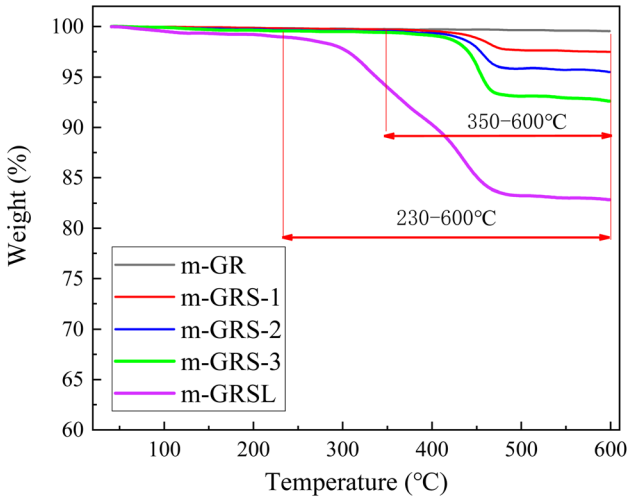

Fig. 6 TGA curves of commercial m-GR, modified m-GRS and m-GRSL.

dispersion is lower, especially the m-GRS-3 dispersion (27.2%), indicating that commercial m-GR was poorly dispersed in water due to its strong van der Waals forces and inherent hydrophobicity, leading to serious agglomeration. Due to the new formed non-covalent π–π interaction between commercial m-GR and SDBS chains, the agglomeration was controlled effectively. As the SDBS content increased, the optical transmittance of m-GR decreased gradually. This trend may occur because higher SDBS content more effectively suppresses tight agglomeration.[6]

However, it is hard to further improve graphene dispersion using non-covalent steric hindrance of small molecule SDBS alone. To achieve both good dispersibility and long-term storage stability simultaneously, the optimized m-GR-3 dispersion was further modified by incorporating LA132 with hydrogen bonding and steric hindrance and electrostatic repulsion. Compared to 27.2% at 550 nm of the optimized m-GR-3 dispersion, the optical transmittance of water-based m-GRSL dispersion is 18.8% in Fig. 3(a), indicating that the dispersibility of m-GRSL has been improved by LA132, as shown in Fig. 1. By comparison, the optical transmittance of the water-based m-GRL dispersion reaches 48.1% in Fig. 3(b), demonstrating that the synergistic modification with SDBS and LA132 is the optimal approach for dispersing commercial m-GR in water.

Furthermore, the optical absorbance spectra reveals the difference between m-GR and modified dispersions in Fig. 3(c), where the former exhibits a characteristic absorption band corresponding to graphene appears at 280 nm.[8] Interestingly, the modified dispersions manifest a slight red-shift for the characteristic absorption peak and also show enhanced absorption peaks. Such spectral changes suggest the π–π stacking interaction between m-GR and SDBS, improving the dispersity of m-GR in water.

3.3 Dispersibility and stability

The zeta potential value is the most crucial parameter characterizing the surface properties of electrostatically stabilized nanomaterials in aqueous solutions.[15] Fig. 4 shows that the zeta potential of the m-GRS dispersion decreases with increasing hydrophilic SDBS content, reaching an absolute value of 33.1 mV for m-GRS-3. However, it remains difficult to prepare the highly homogeneous and stable m-GRS dispersions modified by different SDBS content, indicating that non-covalent steric hindrance interaction provided by small molecule SDBS is still insufficient. To solve this issue, mixed modifiers including SDBS and LA132 were used to functionalize the commercial m-GR. Under optimized conditions, the zeta

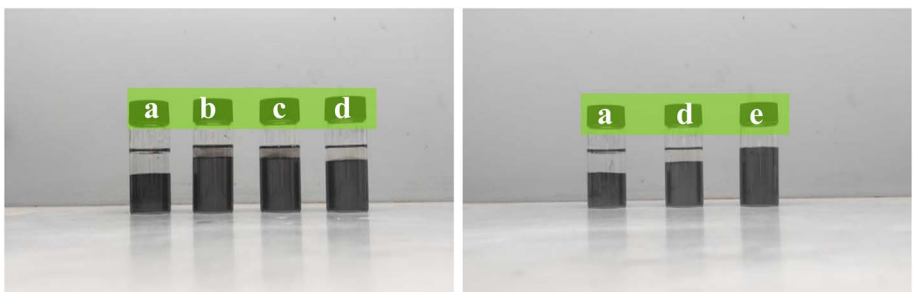

Fig. 5 Comparison photographs of water-based modified m-GR dispersions stored for one month. (a): commercial m-GR, (b): m-GRS-1, (c): m-GRS-2, (d): m-GRS-3, (e): m-GRSL.

potential of the modified m-GRSL dispersion reaches an absolute value of 43.7 mV and maintains good storage stability for one month. The SDBS and LA132-assisted m-GRSL was the most stable dispersion, displaying zeta potentials stronger than ±30 mV, which is a common stability benchmark.[11] More importantly, this modified method is simple and low-cost to achieve large-scale production. Therefore, it can be presumed that both non-covalent steric hindrance interaction and electrostatic repulsion interaction are important factors for preparing a highly homogeneous and stable m-GRSL dispersion. In addition, the absolute value of the water-based m-GRL dispersion is 34.1 mV, indicating that non-covalent steric hindrance interaction of LA132 macromolecule is also insufficient.

In addition, the storage stability of m-GRSL is also much better than that of its completely physical mixture shown in

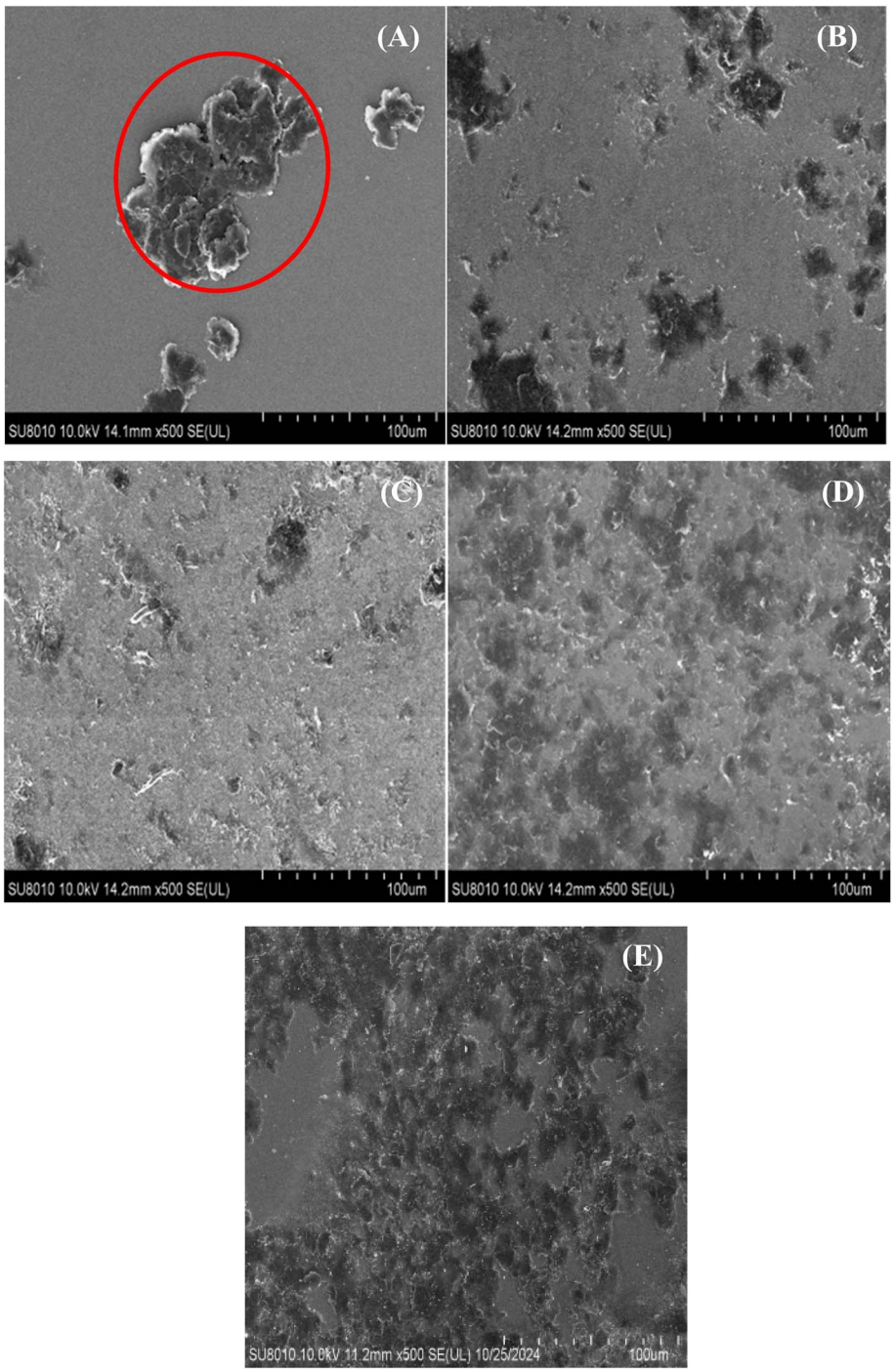

Fig. 7 SEM (A-E) images of commercial m-GR (A), m-GRS-1(B), m-GRS-2 (C), m-GRS-3 (D), and m-GRSL (E) drop-casted from the water solutions.

Fig. 5. Compared with the commercial m-GR, the SDBS and LA132 modified m-GRSL dispersion can be easily dispersed in water, and no sedimentation is observed for one month. The above results demonstrate that the m-GRSL dispersion is a physically stable system and can be considered as an ideal conductive additive for lithium-ion batteries applications.

3.4 TGA measurements

Direct evidence for the non-covalent attachment of the SDBS anionic surfactant and LA132 terpolymer binder to commercial m-GR surfaces comes from thermogravimetric analysis.[15,20] The TGA curves of commercial m-GR, modified m-GRS and m-GRSL at a temperature rate of 10°C min^{-1} are shown in Fig. 6. The TGA curve of commercial m-GR shows a gradual mass loss of around 0.5% as the temperature reaches 600 °C. However, a distinct weight loss region between 350 and 600 °C is observed for modified m-GRS. The results demonstrate that the weight loss of m-GRS increases with higher SDBS modifier content. Compared to commercial m-GR, m-GRS-3 shows a 7.4% weight loss at 600 °C, attributed to the pyrolysis of the SDBS modifier. Furthermore, m-GRSL shows a significant weight loss of around 17.2%, corresponding to the combined pyrolysis of both SDBS modifier and LA132 terpolymer binder. This indicates that both components can be adsorbed onto the graphene surface.

3.5 Surface morphology

It is useful to investigate the influence of different modifiers on the dispersion of m-GR in water because the conductive properties of composites are directly dependent on their dispersion morphology.[15,21] The surface morphologies of commercial m-GR and modified m-GR dispersed in water were examined using SEM, as shown in Fig. 7. The commercial m-GR sheets dispersed in water on the Si substrate show tight agglomeration,[17] which is attributed to their poor dispersion (marked as

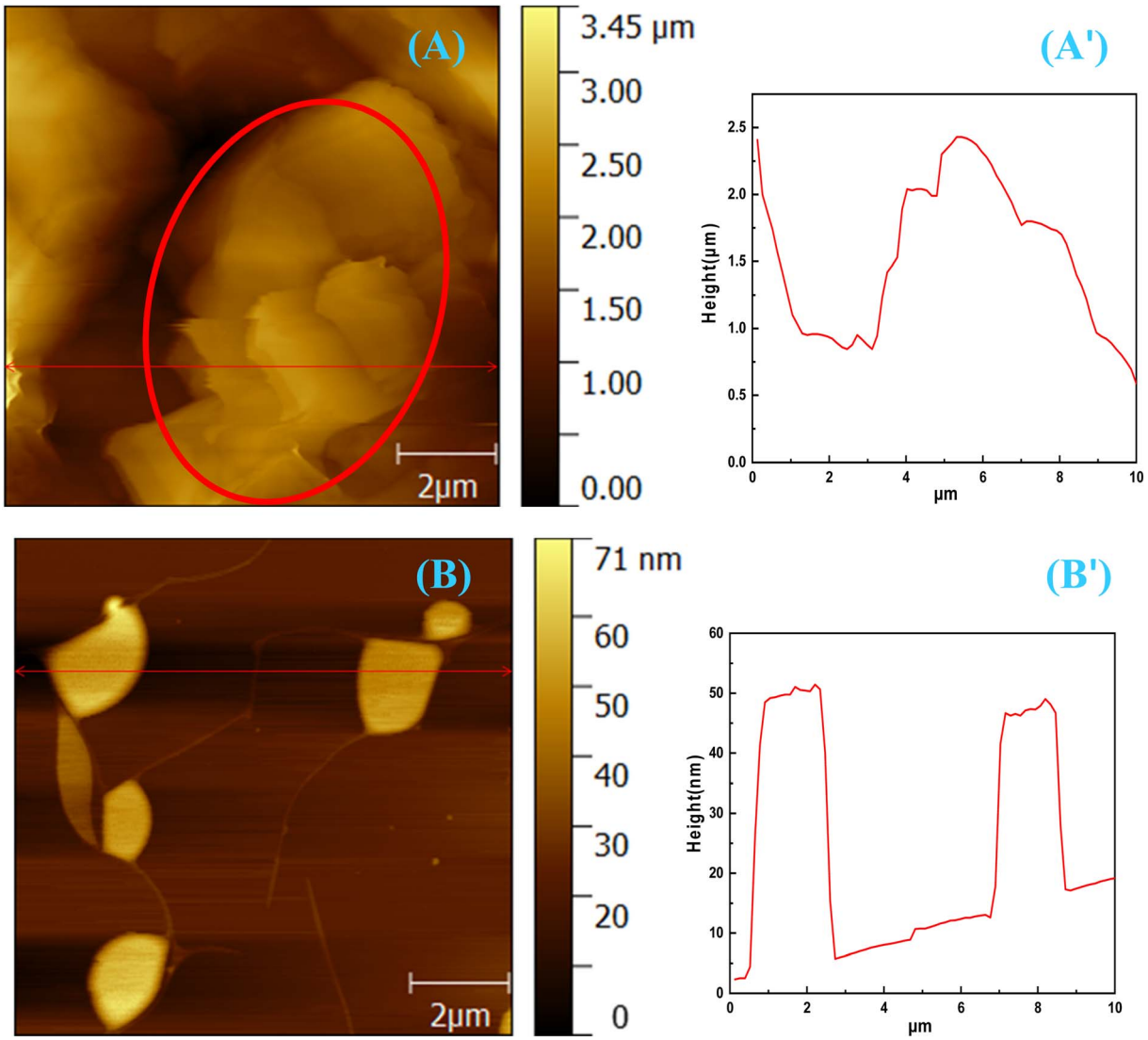

Fig. 8 AFM images of commercial m-GR(A and A′) and modified m-GRSL(B and B′) drop-casted from the water solutions, showing different dispersion morphologies.

red circles in Fig. 7A). In comparison, the aggregation of modified m-GRS is reduced due to SDBS modification. It is evident that the aggregate size of commercial m-GR is reduced. This phenomenon is consistent with m-GRS functionalization *via* non-covalent interaction, where the organic chain can weaken the strong interaction between individual m-GRS sheets. In addition, after modification with SDBS and LA132, the evolution of the uniform morphology is clearly observed. Therefore, we conclude that the optimal water-based m-GRSL dispersion is suitable as a conductive additive for lithium-ion batteries applications.

In addition, AFM results confirmed the dispersibility and thickness of commercial m-GR and modified m-GRSL with the best dispersed stability in Fig. 8. The commercial m-GR dispersed in water show tight agglomeration and exist stacked sheets,[22–26] which is due to the poor dispersion (marked as red circles in Fig. 8A) of m-GR. After the modification with SDBS and LA132, the m-GRSL sheets are well dispersed in water, and show good dispersibility and exist small sheets (Fig. 8B), indicating that the m-GRSL dispersion is easy to disperse in cathode as conductive slurry for water-based lithium-ion batteries. The thickness of commercial m-GR and modified m-GRSL is also examined. As shown in Fig. 8A′, the stacked thickness of the commercial m-GR reaches about 2.5 μm. The thickness of m-GRSL sheets with thin layer is about 50 nm, indicating that the commercial m-GR is dispersed successfully.

3.6 Electronic conductivity

The electronic conductivity of the prepared cathode coating was also measured as a basis for judging the ability of conductive additives to conduct electrons.[27,28] The electronic conductivity of LFP/SP-1 cathode coating with only Super P was 0.074 S cm^{-1} in Fig. 9. After adding the mixed conductive additives with 4 : 1 m-GR and Super P, the electronic conductivity of LFP-m-GR/SP-2 increased to 0.542 S cm^{-1}, indicating that the addition of m-GR could indeed improve the electronic conductivity of LFP/SP cathode materials. By comparison, the electronic conductivity of LFP-m-GRSL/SP-3 reaches higher 0.814 S cm^{-1}, demonstrating that the highly stable modified m-GRSL dispersion can be directly used as a conductive additive in water-based lithium-ion batteries.

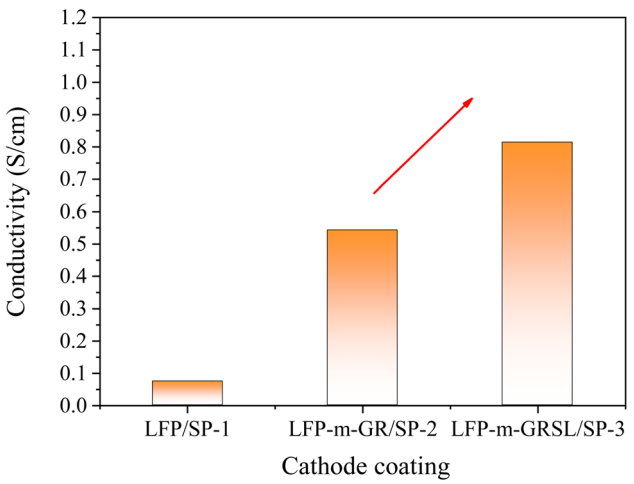

Fig. 9 Electronic conductivity of cathode coating containg different conductive additives.

4. Conclusion

In summary, a highly homogeneous and stable m-GRSL dispersion was successfully prepared in water *via* a low-cost non-covalent surface functionalization technique using commercial m-GR with mixed SDBS and LA132 modifiers. The negative sulfonate group of small molecule SDBS can quickly influence the π–π stacking interaction between the benzene ring and graphene. LA132 is both a macromolecule modifier for m-GR and a binder used in lithium-ion batteries. The results show that the best modified m-GRSL dispersion with the lowest optical transmittance (18.8%) at 550 nm and the largest zeta potential (43.7 mV) can be easily well-dispersed in water, and the aggregates of m-GR are effectively ground into highly dispersed nanosheets using a paint shaker. The m-GRSL dispersion, showing no sedimentation for over one month, has potential application as a functional conductive additive for lithium-ion batteries, providing a new strategy for the high value-added utilization of m-GR.

Conflicts of interest

There are no conflicts of interest to declare.

Data availability

All data generated or analyzed during this study are included in this article.

Acknowledgements

We thank Hefei municipal natural science foundation (No. 202337) and Anhui provincial key research and development program (No. 2023z04020004).

References

1 A. Guerfi, M. Kaneko, M. Petitclerc, M. Mori and K. Zaghib, *J. Power Sources*, 2017, **163**, 1047.
2 M. H. Sun, H. X. Zhong, S. R. Jiao, H. Q. Shao and L. Z. Zhang, *Electrochim. Acta*, 2014, **127**, 239.
3 J. T. Li, Z. Y. Wu, Y. Q. Lu, Y. Zhou, Q. S. Huang, L. Huang and S. G. Sun, *Adv. Energy Mater.*, 2017, **7**, 1701185.
4 H. Xiao, J. T. Zhao, Q. Gao, W. J. Zhang, X. Cheng, C. Y. Song and G. X. Li, *Chem. Eng. J.*, 2025, **506**, 159927.
5 I. Nagore, L. Gabriele, P. Alessandro, G. Claudio, M. David, L. Jalel and L. Kraft, *ACS Appl. Polym. Mater.*, 2025, **7**(6), 3764.
6 A. O. Borode, N. A. Ahmed and P. A. Olubambi, *Int. J. Thermophys.*, 2021, **42**, 158.
7 Y. Lu, F. Yang, G. G. X. Wang, T. Y. Zhang and P. Wang, *Int. J. Electrochem. Sci.*, 2019, **14**, 5961.

8 Y. Wen, H. M. Liu and X. Y. Jiang, *Mater. Sci. Eng. B.*, 2023, **297**, 116764.
9 Y. Shi, L. Wen, S. F. Pei, M. J. Wu and F. Li, *J. Energy Chem.*, 2019, **30**, 19.
10 D. W. Johnson, B. P. Dobson and K. S. Coleman, *Curr. Opin. Colloid Interface Sci.*, 2015, **20**, 367.
11 D. Parviz, S. Das, H. S. T. Ahmed, F. Irin, S. Bhattacharia and M. J. Green, *ACS Nano*, 2012, **6**, 8857.
12 Y. J. Wu, R. H. Tang, W. C. Li, Y. Wang, L. Huang and L. Z. Ouyang, *J. Alloy Compd.*, 2020, **830**, 154575.
13 C. Zapata-Hernandez, G. Durango-Giraldo, D. López, R. Buitrago-Sierra and K. Cacua, *J. Disper. Sci. Technol.*, 2021, **43**(11), 1717.
14 M. H. Li, Z. Q. Du, X. T. Fang, X. J. Ge and S. J. Yu, *J. Nanopart. Res.*, 2023, **25**, 216.
15 M. H. Li, X. Y. Lu, J. J. Jiang, L. Gao, J. Gao and D. M. Jiang, *RSC Adv.*, 2022, **12**, 6037.
16 Y. He, C. L. Chen, G. Q. Xiao, F. Zhong, Y. Q. Wu and Z. He, *React. Funct. Polym.*, 2019, **137**, 104.
17 Y. Feng, L. Camilli, T. Wang, D. M. A. Mackenzie, M. Curioni, R. Akid and P. Boggild, *Carbon*, 2018, **132**, 78.
18 M. H. Li, X. J. Ge, P. Wu, H. Chu and Z. Li, *J. Nanopart. Res.*, 2025, **27**, 20.
19 M. H. Li, D. M. Jiang, Q. Du, Z. S. J. Yu, X. J. Ge and Y. He, *J. Nanopart. Res.*, 2023, **25**, 85.
20 M. H. Li, Z. Y. Xu, J. Y. Chen and S. E. Zhu, *J. Polym. Eng.*, 2018, **38**(6), 537.
21 S. Wang, Z. R. Hu, J. Shi, G. K. Chen, Q. Zhang, Z. S. Weng, K. Wu and M. G. Lu, *Appl. Surf. Sci.*, 2019, **484**, 759.
22 D. Li, M. B. Müller, S. Gilje, R. B. Kaner and G. G. Wallace, *Nat. Nanotechnol.*, 2008, **3**, 101–105.
23 X. Xu, D. Yi, Z. Wang, J. Yu, Z. Zhang, R. Qiao, Z. Sun, Z. Hu, P. Gao, H. Peng, Z. Liu, D. Yu, E. Wang, Y. Jiang, F. Ding and K. Liu, *Adv. Mater.*, 2018, **30**, 1702944.
24 W. Sun, T. Wu, L. Wang, Z. Yang, T. Zhu, C. Dong and G. Liu, *Compos. Part B-Eng.*, 2019, **173**, 106916.
25 N. Zhang, P. Ma, Z. L. Yang, Y. C. Fang and Z. Y. Zhang, *J. Superhard Mater.*, 2023, **45**, 186–191.
26 Z. Y. Xiong, L. Y. Shen, J. Long, X. Li, K. Zhou, G. M. Choi, K. T. Ou, G. Y. Yang, W. C. Ma, H. S. Lee, Y. Y. Sun and D. Li, *Nat.Commun.*, 2024, **15**, 10807.
27 T. Liu, S. M. Sun, Z. Zang, X. C. Li, X. L. Sun, F. T. Cao and J. F. Wu, *RSC Adv.*, 2017, **7**, 20882.
28 W. C. Chien, Y. R. Li, S. H. Wu, Y. S. Wu, Z. H. Wu, Y. J. Li and C. C. Yang, *Adv.Powder Technol.*, 2020, **31**, 4541–4551.